RASĀYAN *J. Chem.*
Vol. 15 | No. 3 |2148-2154| July - September | 2022
ISSN: 0974-1496 | e-ISSN: 0976-0083 | CODEN: RJCABP
http://www.rasayanjournal.com
http://www.rasayanjournal.co.in

PERFORMANCE EVALUATION OF GRAPHENE (CTAB)/TIO_2/Fe_3O_4 COMPOSITE ON PHENOL DEGRADATION

D. Heltina✉, D. G. Randa, M. B. A. Naufal, A. Partama, and Komalasari
Department of Chemical Engineering, Riau University, Pekanbaru-28293, Riau, Indonesia
✉Corresponding Author: desi.heltina@lecturer.unri.ac.id

ABSTRACT

Experimental and theoretical studies on the phenolic degradation of graphene (CTAB)/TiO_2/Fe_3O_4 have been conducted. The addition of surfactant cetyltrimethylammonium bromide surfactant (CTAB) on graphene can improve the performance and dispersion of TiO_2 on the graphene surface and prevent electron recombination. Magnetic materials such as Fe_3O_4 will help the composite separation process, but will also have an effect on its photodegradation performance. The effect of Fe_3O_4 composition on composites was characterized using Scanning Electron Microscope, X-Ray Diffraction, FT-IR Spectra, Brunaeuer Emmett Teller-BJH, UV-Vis DRS, and UV-vis Spectrophotometer analysis. Furthermore, the photodegradation of phenol was carried out under visible light irradiation to investigate the photocatalytic activity. TiO_2 nanoparticles doped with graphene (CTAB) have a large enough synergistic effect, besides that graphene nanocatalyst (CTAB)/TiO_2/Fe_3O_4 is more efficient because it is easy to separate.

Keywords: Photodegradation, Magnetic composite, TiO_2, Graphene, CTAB, Phenol.
RASĀYAN *J. Chem.*, Vol. 15, No.3, 2022

INTRODUCTION

Phenol compounds are industrial wastes that contain benzene rings[1], and they can be removed from wastewater through electrochemical, catalytic, biological, and adsorption methods.[2] These developed wastewater treatment methods still have weaknesses, therefore, the photocatalyst is an alternative method used to solve environmental problems.[3] Photocatalysis is a technique that uses hydroxyl radicals with strong selectivity and reactivity with different pollutants, as shown by the value of its degradation rate, which ranges from 10^6 to 10^9 mol/L/s.[4] The use of titanium dioxide (TiO_2) semiconductors in mineral form or composite systems have become a major concern in the application of photocatalysis for the degradation of chemical pollutants.[5] Besides, the consolidation of graphene in titanium dioxide can influence the surface region, pore volume, and crystal size. This increases the adsorption rate of the photodegradation action in the decomposition of aqueous solutions.[6] The addition of surfactants provides a good synergistic effect between TiO_2 and graphene as well as increases the number of active sites of the composite.[7] Graphene compounds can be dissolved in water by non-covalent interaction with surfactants like as sodium dodecyl sulfate (SDS) and cetyltrimethylammonium bromide (CTAB).[8] Modification of graphene using CTAB surfactants can prevent agglomeration of TiO_2 particles to enhance their distribution on the graphene surface.[9] The application of TiO_2/graphene (CTAB) photocatalyst is limited by the difficulty in the disjunct of the catalyst material after the photodegradation process has been conducted. Recently, the recovery of photocatalyst nanoparticles based on titania-graphene has been widely developed, including the use of magnetic compounds. The incorporation of magnetic components prevents the agglomeration of catalyst particles during recovery and increases the durability through the application of an appropriate magnetic field. The magnetically modified composite TiO_2-Graphene (CTAB)/Fe_3O_4 becomes one that is an intriguing topic. The main objective of this study is to investigate the properties of magnetic composites and their various uses in wastewater treatment. The magnetic composites were also subjected to a magnetic separation test to show the potential of magnetic composites that will be recovered.[10]

EXPERIMENTAL

The materials used are graphene obtained from Hongwu Int'l Group Ltd., TiO_2 P25 (Evonik) Degussa, *Cethyltrimethylammonium Bromide* (CTAB), Nitric Acid (HNO_3), Iron (III) Chloride Hexahydrate

http://doi.org/10.31788/RJC.2022.1536857

($FeCl_3.6H_2O$), Iron (II) Chloride Tetrahydrate ($FeCl_2.4H_2O$), Hydrochloric Acid (HCl), Ammonium Hydroxide (NH_4OH) and aqua dest.

Graphene Changes with CTAB (grapheme/CTAB)
In a 100 ml aqua dest, 1 g graphene and 0.5 g CTAB were combined and sonicated for 1 hour. Additionally, the liquid was strained with a vacuum pump to generate a solid suspension, which was then dried at 110 ^oC to yield graphene (CTAB).

Synthesis of Fe_3O_4
In 5.15 ml of HCl 0.1 N, 2.6 g of $FeCl_3.6H_2O$ and 1 g of $FeCl_2.4H2O$ were dispersed and agitated until the solid was completely dissolved. The ferric salt solution was then diminished with 7.5 mL aqua dest and agitated for 15 minutes at 300 rpm with a stirrer. In addition, 135 ml of NH_4OH 1.5 N was added, and a black-colored solution was obtained after 1 hour of stirring at 300 rpm with a magnetic stirrer. Until pH 7, the solution was rinsed with aqua dest and separated with an external magnet. The solid solution was then dried at 100 degrees Celsius, and the result was ground to yield Fe_3O_4 in powdered.

Synthesis of Graphene (CTAB)/TiO_2/Fe_3O_4 Composite
To alter the content of Fe3O4 in the composite TiO2/graphene (CTAB)/Fe_3O_4, the synthesized Fe_3O_4 was taken as 0.3, 0.5, and 0.7 g. Meanwhile, 100 ml aqua dest was combined with 1 g TiO_2 and 0.1 g graphene (CTAB), and pH 3 was achieved by injecting HNO_3 into the mixture. After stirring for 30 minutes at 300 rpm with a magnetic stirrer, the mixture was sonicated for 30 minutes. By adding 0.3, 0.5, and 0.7 g of Fe_3O_4 to the mixture, graphene (CTAB)/TiO_2/Fe_3O_4 (GTF) composites were created. In addition, the mixture was stirred and sonicated for 30 minutes before being dried at 100°C. The sample was calcined for 2 hours at 400°C in a nitrogen environment, then crushed to get graphene (CTAB)/TiO_2/Fe_3O_4 powder.

Performance Test of Graphene (CTAB)/TiO_2/Fe_3O_4 Composites Using Phenol Compound
The observation was done for 4 hours with a photon source that used 250 watts of mercury lamp, and a 0.3 g composite sample of graphene (CTAB)/TiO_2/Fe_3O_4 was introduced to 10 ppm of 300 ml of phenol liquid. The photocatalytic degradation was carried out in a photoreactor sized 40 cm by 50 cm by 60 cm. Meanwhile, the photocatalyst employed in the experiment was a 0.3 g powder that was agitated to produce particles of photocatalyst and phenol in the solution. The result of deteriorated phenol was obtained using a UV-Vis Spectrophotometer in compliance with the accordance method.

Magnetic Separation Analysis of Graphene (CTAB)/TiO_2/Fe_3O_4 Composites
The beaker glass that contains phenol and graphene (CTAB)/TiO_2/Fe_3O_4 composite solution was placed above an external magnet for a magnetic separation test. The composites may be reused for photodegradation after being separated, and images were taken at intervals till all the particles were totally separated from the solution.

Characteristic
Scanning Electron Microscope, X-Ray Diffraction, FT-IR Spectra, Brunaeuer Emmett Teller-BJH, UV-Vis DRS, and UV-vis absorption spectroscopy were used to describe the sample.

RESULTS AND DISCUSSION

Functional groups of graphene (CTAB)/ TiO_2/Fe_3O_4 composites were analyzed by FT-IR spectra. Figure-1 showed the FT-IR spectra of samples TiO_2, graphene (CTAB), Fe_3O_4, and TiO_2/Graphene (CTAB)/Fe_3O_4. At a wavelength of 3400 cm^{-1} O-H bonds showed that the surface of the photocatalyst adsorb the water molecules[11] and the wavelength of 705.01 cm^{-1} showed Ti-O-Ti bonds from titanium dioxide.[12] Furthermore, the wavelength of 2850 cm^{-1} showed Ti-O-C bonds between TiO_2 and graphene[13] while Fe-O bonds were in the wavelength of 635.57 cm^{-1} from Fe_3O_4.
To determine the crystallinity and size of the Graphene (CTAB)/ TiO_2/Fe_3O_4 composite, an XRD test was conducted as seen in Fig.-2, and the results for the graphene (CTAB)/TiO_2/Fe_3O_4 composite showed that TiO_2 anatase appears at an angle of 2θ=25.2552°; 48.0363°; 53.9296°; 62.7248°. The position of the main peak of TiO_2 anatase is at an angle of 2θ = 25.2552° with a peak height of 329.30 counts. This is

consistent with the results from the International Center for Diffraction Data (ICDD) for TiO_2 anatase with hkl (101); (200); (105); (204). Furthermore, the crystal size was obtained using the Scherrer equation, which was 19.72 nm.

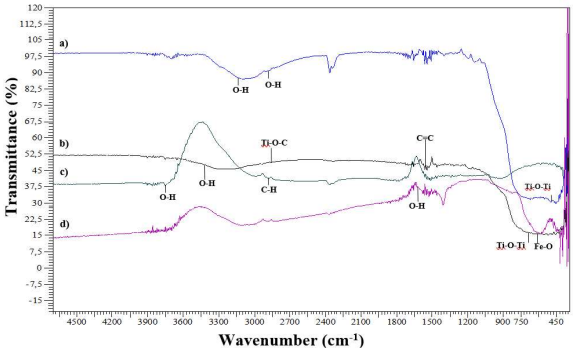

Fig.-1: Fourier-Transform Infrared Spectroscopy Spectra of (a) TiO_2, (b) graphene (CTAB)/TiO_2/Fe_3O_4, (c) graphene (CTAB), (d) Fe_3O_4

Rutile TiO_2 has hkl value similar to the characterization pattern of rutile TiO_2 XRD analysis with ICDD data standards, namely (110); (101); (110) with angle 2θ = 26.4671°; 35.5911°; 27.4095°. The main peak position of rutile TiO_2 is at an angle of 2θ = 26.4671° with a peak height of 64.67 counts and crystal size obtained using the Scherrer equation of 22.91 nm. The fractions for anatase and rutile TiO_2 were 80% and 20%, respectively, and their composition created a synergistic electron transfer that can increase the activity of electron-hole transfer and photocatalytic activity compared to composites of one phase.[14] In addition, composites that have anatase and rutile compositions can prevent the recombination process.[15] There are also magnetite peaks that have hkl values similar to the standard XRD magnetite characterization pattern of ICDD data, namely (511); and (220) with an angle of 2θ = 57.363°; and 30.288°. This indicates that Fe_3O_4 successfully binds to graphene (CTAB)/TiO_2. The crystallinity of magnetite is 16.33 nm from the calculations using the Scherrer equation. The peaks in the graphene (CTAB)/TiO_2/Fe_3O_4 composite were not found, because the TiO_2 composition was higher. Therefore, the small TiO_2 particles covered the graphene (CTAB) components in the diffraction peak XRD analysis.[16]

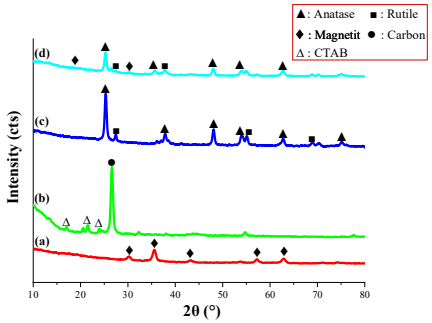

Fig.-2: XRD Pattern of (a) Fe_3O_4; (b) *Graphene*-CTAB; (c) TiO_2; d) Composite Graphene (CTAB)/TiO_2/Fe_3O_4

Figure-3 showed the morphology of TiO_2, Graphene (CTAB), Fe_3O_4, and graphene (CTAB)/TiO_2/Fe_3O_4 composite was characterized using SEM. Figure-3 (d) TiO_2 particles are evenly distributed on the surface of graphene-modified with CTAB (Cetyltrimethylammonium bromide) surfactant. Graphene modification using CTAB surfactant distributes TiO_2 on the graphene surface.[9]

Table-1 showed that graphene (CTAB)/TiO_2/Fe_3O_4 composites have a larger surface area than TiO_2 P25 and TiO_2/Fe_3O_4. The addition of graphene material will increase the surface area of the composite[6] and this can have an impact on composite performance during the photodegradation of organic substances. The increased proportionality of the surface area and the contact between the reactants and the composite surface helps to degrade more organic compounds. Modification of graphene using CTAB surfactants can prevent agglomeration of TiO_2 particles to enhance their distribution on the graphene surface.[9] The addition of Fe_3O_4 can reduce the surface area of the composite so that it can cause a decrease in the photodegradation activity of phenolic compounds. This is the possible shading effect that occurs in

composite materials. The shading effect is the effect caused by other compounds that can cover the surface area of TiO_2 which can block the photon source.[17]

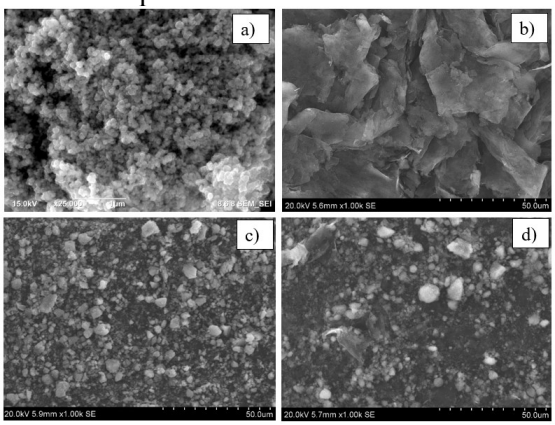

Fig.-3 : Morphology of (a) TiO_2, (b) Graphene, (c) Fe_3O_4, and (d) Graphene (CTAB)/TiO_2/Fe_3O_4

Table-1: Specific Surface Area of Materials

Material	Surface Area (m^2/g)
TiO_2 P25	54.93
Graphene*e*-CTAB/TiO_2	64
TiO_2/Fe_3O_4	53.41
Graphene (CTAB)/TiO_2/Fe_3O_4	57.34

The BJH method (Barrett, Joyner, and Halenda) is used to determine the distribution of pore size, diameter, and length.[18] Based on the results of the N_2 adsorption-desorption analysis shown in Fig.-4 it is known that the isotherm type of graphene (CTAB)/TiO_2/Fe_3O_4 composite material is a type IV with a hysteresis loop H3 with the pore size is 33.8 Å or 3.38 nm. Type IV is a mesoporous characterized by the presence of a hysteresis loop due to volume differences. N_2 is adsorbed and desorbed since the graphene (CTAB)/TiO_2/Fe_3O_4 composite is a mesoporous material with a pore size of 2 - 50 nm.[19]

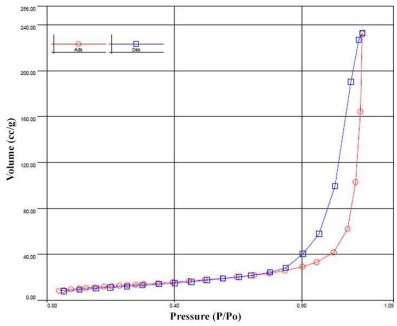

Fig.-4: Composite N_2 Adsorption-Desorption Isotherm Curve of Graphene (CTAB)/TiO_2/Fe_3O_4 composite

UV-Visible Diffuse Reflectance Spectra characterization is utilized to calculate the energy band gap of composite materials. Furthermore, band gap energy value is important for semiconductor materials. This is because energy is one of the factors that affect the performance of semiconductors in electron and hole transfer.[20] Figure-5 showed diffuse reflectance spectra and Kubelka-Munk plots for band gap calculation. The bandgap energy of composite materials can be measured by the Kubelka-Munk equation. Table-2 showed the energy band of composite materials, and the addition of graphene (CTAB) to the composite can cause a narrowing of the bandgap energy. Therefore, the light absorption is included in the visible range with a wavelength above 400 nm, and this has been proven by the Ti-O-C bonds in the FT-IR analysis.

Photocatalytic Activity

The mass variation of Fe_3O_4 including 0.3, 0.5, and 0.7 g composite was used to degrade phenol. After the photodegradation process was completed, the absorbance value of the phenol solution was estimated

using a UV-Vis spectrophotometer with a wavelength of 500 nm. Figure-6 showed a decrease in the concentration of phenol with increasing photodegradation time.

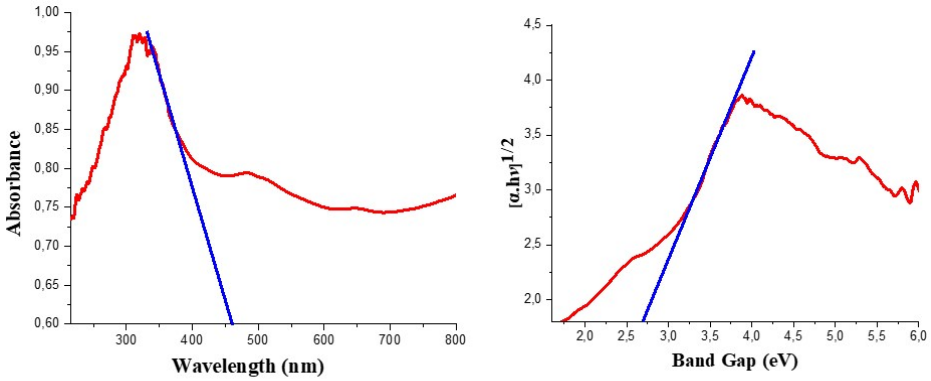

a) b)

Fig.-5: DRS (a) and Kubelka–Munk Plots for Band Gap Calculation (b)

Table-2: Wavelength and Band Gap Value of Photocatalyst Materials

Material	Wavelength (nm)	Eg(eV)
TiO_2 P25	378	3.28
Graphene (CTAB)/TiO_2/Fe_3O_4	460	2.7

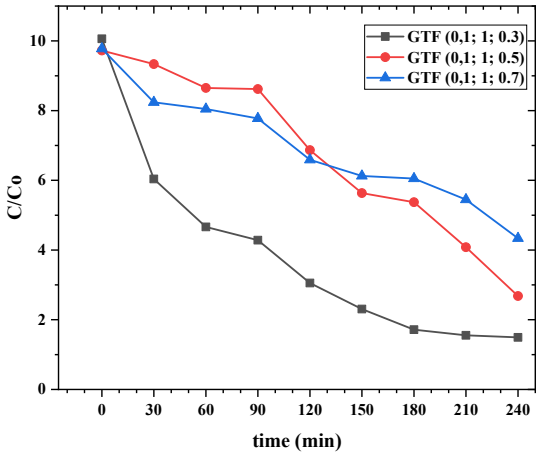

Fig.-6: The Relative Concentration (C/Co) of Phenol versus Time

Figure-7 showed an inverse relationship between the percentages of phenol degradation with a mass variation of Fe_3O_4. This is due to Fe_3O_4 particles distributed across the composite surface covering the TiO_2 surface. The more Fe_3O_4 composition in the composite, the more TiO_2 surface covered by Fe_3O_4 particles. Thusly, TiO2 doesn't get sufficient light to initiate the photocatalyst. Fewer hydroxyl radicals (•OH) are formed with the lack of photon sources that affect the active site of the photocatalyst, and this reduced the composite ability in the phenol photodegradation process.

Magnetic Separation Test

Table-4 showed the results of magnetic separation on Graphene (CTAB)/TiO_2/Fe_3O_4 composites after placing the composite solution on a bar magnet and calculating the separation process time. The more Fe_3O_4 is contained in the Graphene (CTAB)/TiO_2/Fe_3O_4 composite, the faster the magnetic separation in the solution. This is because the Fe_3O_4 mass in the composite is spread over the surface of the composite to increase the magnetic response throughout the surface.[21]

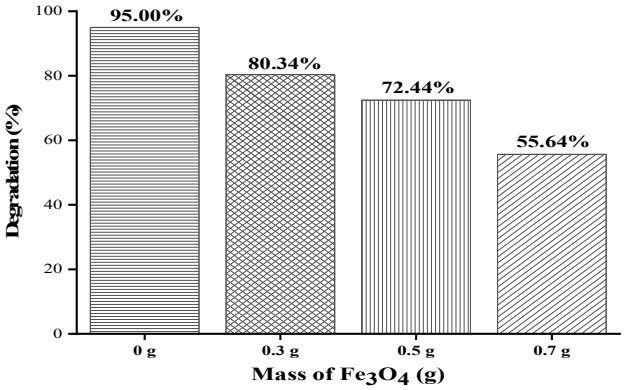

Fig.-7: Photocatalytic Activity of Graphene (CTAB)/TiO_2/Fe_3O_4 Composite with Variation Mass of Fe_3O_4

Table-4: Magnetic Separation Test

Mass of Fe_3O_4	Time (min)				
	0	10	20	30	40
0,3 g					
0,5 g	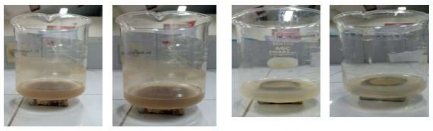				
0,7 g	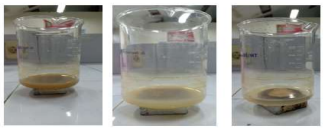				

Recycling of Graphene (CTAB)/TiO_2/Fe_3O_4

The Graphene (CTAB)/TiO_2/Fe_3O_4 composite was reused for the photodegradation process to determine the performance of the Graphene (CTAB)/TiO_2/Fe_3O_4 composite. Percentage degradation for two repetitions in a row is 75.54% and 73.50%. The results of the repetition of Graphene (CTAB)/TiO_2/Fe_3O_4 composites can be seen in Fig.-8.

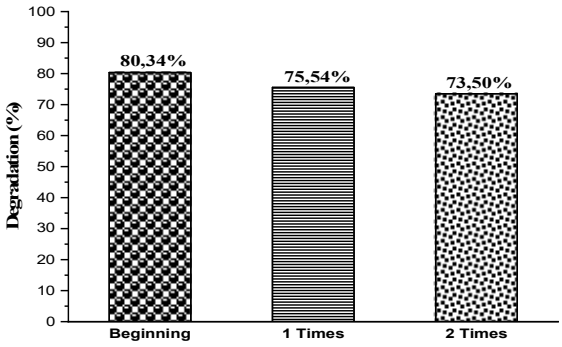

Fig.-8: Recycling Ability of Graphene (CTAB)/TiO_2/Fe_3O_4

CONCLUSION

Graphene (CTAB)/TiO_2/Fe_3O_4 composites have been successfully synthesized by mixing and evaporation methods. A photodegradation activity test was conducted in degrading phenol, and the results showed that the TiO_2 doped graphene (CTAB) nanoparticles have a considerable synergistic effect that can increase photocatalytic activity. Furthermore, the higher the mass of Fe_3O_4 in the composite, the less efficient the photocatalyst is in reducing phenol and the faster the separation.

ACKNOWLEDGEMENT

The authors are thankful for the financial assistance of this study (Hibah) Penelitian Dasar, no. 482/UN.19.5.1.3/PT.01.03/2021, from the DRPM Universitas Riau and the Indonesian Ministry of National Education's Directorate General of Higher Education (DGHE).

REFERENCES

1. F. Chang, Z. Chen, J. Jing and J. Hou, *Journal of Materials Chemistry C* , **8(9)**, 3000(2020), https://doi.org/10.1039/C9TC05010H
2. O. Israa, M. A. Hajja, I. Ismail, J. H. Zain and F. Banat, *Materials Chemistry and Physics,* **238**, 121931(2019), https://doi.org/10.1016/j.matchemphys.2019.121931
3. N. Chiaki, Y. Asakura, K. Shiraki, A. Yamakata and S. Yin, *Chemical Engineering Journal*, **390**, 124616(2020), https://doi.org/10.1016/j.cej.2020.124616
4. V. Priya, S. K. Krishna, V. Sivakumar, and P. Sivakumar, *Rasayan Journal of Chemistry,***12(3)**, 1361 (2019), http://dx.doi.org/10.31788/RJC.2019.1235189
5. K. Rafal, J. Musial, P. Bakun, M. Spychala, B. Czarczynska-Goslinska, D. T. Mlynarczyk, T. Koczorowski, L. Sobotta, B. Stanisz and T. Goslinski, *Applied Sciences*, **11(18)**, 8674(2021), https://doi.org/10.3390/app11188674
6. K. Nejman, Ewelina, A.Wanag, J. Kapica-Kozar, Ł. Kowalczyk, M. Zgrzebnicki, B. Tryba, J. Przepiorski and W. Morawski, *Catalysis Today*, **357**, 630(2020), https://doi.org/10.1016/j.cattod.2019.04.078
7. Hu, Ju, H. Li, S. Muhammad, Q. Wu, Y. Zhao and Q. Jiao, *Journal of Solid State Chemistry*, **253**, 113(2017), https://doi.org/10.1016/j.jssc.2017.05.034
8. Subrahmanyam, Vivekchand, A. Govindaraj and Rao, *Journal of Materials Chemistry*, **13**, 1517(2008), https://doi.org/10.1039/b716536f
9. C. Gang, S. Ouyang, Y. Deng, M. Chen, Y. Zhao, W. Zou and Q. Zhao, *The Royal Society of Chemistry advances*, **32**, 18652(2019), https://doi.org/10.1039/C9RA03250A
10. X. Shouhu, W. Jiang, X. Gong, Y. Hu and Z. Chen, *The Journal of Physical Chemistry C*, **113**, 553(2009), https://doi.org/10.1039/C2DT12307J
11. Nadimi, Z. Saravani, Aroon and E. Pirbazari, *Materials Chemistry and Physics*, **225**, 464 (2019), https://doi.org/10.1016/j.matchemphys.2018.11.029
12. Z. Lixin, J. Zhang, H. Jiu, C. Ni, X. Zhang and M. Xu, *Journal of Physics and Chemistry of Solids*, **86**, 82(2015), https://doi.org/10.1016/j.jpcs.2015.06.018
13. Z. Fatemah, M. Reza, A. Yazdi and M. Eslamian, *Catalysts*, **7**, 136(2017), https://doi.org/10.3390/catal7050136
14. Siah, W. Ruu, H. O. Lintang, M. Shamsuddin and L. Yuliati, *IOP Conference Series: Materials Science and Engineering*, **107**, 012005(2016), https://doi.org/10.1088/1757-899X/107/1/012005
15. Hurum, Deanna, C.Alexander, G. Agrios, Kimberly, A. Gray, T. Rajh and M. C. Thurnauer, *The Journal of Physical Chemistry B*, **107(19)**, 4545(2003), https://doi.org/10.1021/jp0273934
16. N. R. Khalid, E. Ahmed, Z. Hong, L. Sana, and M. Ahmed, *Current Applied Physics*, **13**, 663(2013), https://doi.org/10.1016/j.cap.2012.11.003
17. D. Beketova, M. Motola, H. Sopha, J. Michalicka, V. Cicmancova, F. Dvorak, L. Hromadko, B. Frumarova, M. Stoica and J. M. Macak, *American Chemical Society Applied Nano Materials*, **3(2)**, 1553(2020), https://doi.org/10.1021/acsanm.9b02337
18. V. Rocha, Jhinnym D. Barrera and K. Sapag, *Microporous and Mesoporous Materials*, **200**, 68(2014), https://doi.org/10.1016/j.micromeso.2014.08.017
19. K. Katsumi, *Journal of membrane science*, **96**, 58(1994), https://doi.org/10.1016/0376-7388(94)00126-X
20. L. Diah, W. Sunarto and E. B. Susatyo, *Indonesian Journal of Chemical Science*, **1**, 1(2012), https://doi.org/10.15294/ijcs.v1i1
21. Slamet, P. P. D. K. Wulan, D. Heltina, A. Fisli and D. Philo, *Journal of Physics: Conference Series*, **1091**, 012024(2018), https://doi.org/10.1088/1742-6596/1091/1/012024

[RJC-6857/2021]